Vol 18 No 6, June 2009
1674-1056/2009/18(06)/2393-05

Chinese Physics B

© 2009 Chin. Phys. Soc.
and IOP Publishing Ltd

High-performance evanescently-coupled uni-traveling-carrier photodiodes*

Zhang Yun-Xiao(张云霄)†, Liao Zai-Yi(廖栽宜), and Wang Wei(王 圩)

Key Laboratory of Semiconductor Materials Science, Institute of Semiconductors, Chinese Academy of Sciences, Beijing 100083, *China*

(Received 22 October 2008; revised manuscript received 10 November 2008)

A new evanescently-coupled uni-traveling-carrier photodiode (EC-UTC PD) based on a multimode diluted waveguide (MDW) structure is fabricated, analysed and characterized. Optical and electrical characteristics of the device are investigated. The excellent characteristics are demonstrated such as a responsivity of 0.36 A/W, a bandwidth of 11.5 GHz and a small-signal 1-dB compression current greater than 18 mA at 10 GHz. The saturation current is significantly improved compared with those of similar evanescently-coupled pin photodiodes. The radio frequency (RF) bandwidth can be further improved by eliminating RF losses induced by the cables, the probe and the bias tee between the photodiode and the spectrum analyzer.

Keywords: evanescently-coupled uni-traveling-carrier photodiode, multimode diluted waveguide, beam propagation method, 1-dB compression current

PACC: 4280L, 4280S, 2940P

1. Introduction

There is an increasing demand for photodiodes (PDs) with a high output and a wide bandwidth because they can allow us to simplify the configuration of receivers for broadband fiber-optic communications and ultra fast measurement systems. High-speed photodetectors are key devices in the fields of digital, analogue, and optical transmissions. A uni-traveling-carrier photodiode (UTC-PD)[1−4] is a promising device because it has a higher output and a faster response than the conventional pin PDs, owning to its unique operation mode.[1] Most of the UTC photodiodes have been realized by using surface illuminated structures. However, the tradeoff between quantum efficiency and transit time for surface PDs restricts the responsivity. Edge illuminated waveguide photodetectors can circumvent the tradeoff between high quantum efficiency and short transit time.[5] However, a high power input of several mW will cause saturation, even damage at the front end of the waveguide. Evanescent edge coupled waveguide PDs, of which the saturation current is four times higher than that of PDs made through a side-illuminated approach[6] due to their more uniform light absorption structure, have been used widely because such a PD structure (bandwidth) and fiber-device coupling (external quantum efficiency and high power handling capability) can be designed independently, and they can be useful for both high optical responsivity and high power.[7−10] We have put forward a novel optical gates scheme in which a short planar diluted waveguide uni-traveling carrier (SPMW UTC) photodiode is integrated with an electroabsorption modulator (EAM) with a large optical cavity (LOC) structure.[11]

In the present paper, we report on new evanescently-coupled uni-traveling-carrier photodiodes (EC-UTC PDs) combined with a multimode diluted waveguide (MDW) structure.[12] The MDW contains five $Q_{1.2}$ layers alternating with five InP layers and two optical matching layers ($Q_{1.2}$ and $Q_{1.4}$). Such a design has proven simultaneous high responsibility, large bandwidth and high-output characteristics. A high responsibility of 0.36 A/W at 1.55 μm without an anti-reflection coating, –1 dB compression current of more than 18 mA, together with more than 11.5 GHz

*Project supported by the National High Technology Research and Development of China (Grant Nos 2006AA01Z256, 2007AA03Z419 and 2007AA03Z417), the State Key Development Program for Basic Research of China (Grant Nos 2006CB604901 and 2006CB604902), and the National Natural Science Foundation of China (Grant Nos 90401025, 60736036，60706009 and 60777021).

†E-mail: zhangyx@semi.ac.cn

bandwidth are demonstrated by using the structure.

2. Structure design and fabrication

Figures 1(a) and 1(b) show the schematic cross sectional and top views of the EC-UTC TWPD, respectively. The structure was grown by metal organic chemical vapour deposition (MOCVD) on a semi-insulating (SI) substrate. The 25-μm-long input waveguide comprised an MDW (composed of five $Q_{1.2}$ layers with 115-, 158-, 200-, 240-, and 280-nm thicknesses alternating with five 120-nm-thick InP layers), a 320-nm-thick n^+-doped $Q_{1.2}$ optical matching layer and a 300-nm-thick undoped $Q_{1.4}$ optical matching layer. The absorbing superstructure was made of a 0.15-μm–thick p-doped $Q_{1.57}$ absorbing layer, a 0.35-μm-thick p^+-doped InP layer, and a p^+-doped InGaAs contact layer. The unique feature of the EC-UTC-PD was that the undoped $Q_{1.4}$ optical matching layer was simultaneously used as the undoped carrier collector layer, which could improve the epitaxial quality because the growth of the extra epi-layer was suppressed. The input passive waveguide and the active waveguide were designed to have the same width (6 μm) simplifying the fabrication process. Evanescently coupled waveguide structures of the photodiodes were patterned by using dry etching, followed by a wet etching. The SiO2 was used as an anti-etching mask and a thin InP layer on the top of the multimode waveguide served as an etch stop layer. A SiO_2 passive film was then deposited. After the diode was isolated by a dry etch, a planarization polyimide was patterned where the electrical pads were finally formed. As shown in Fig.1(b), a coplanar waveguide, which was connected with an active area of photodiode, was fabricated on a SI InP substrate for a high-speed measurement.

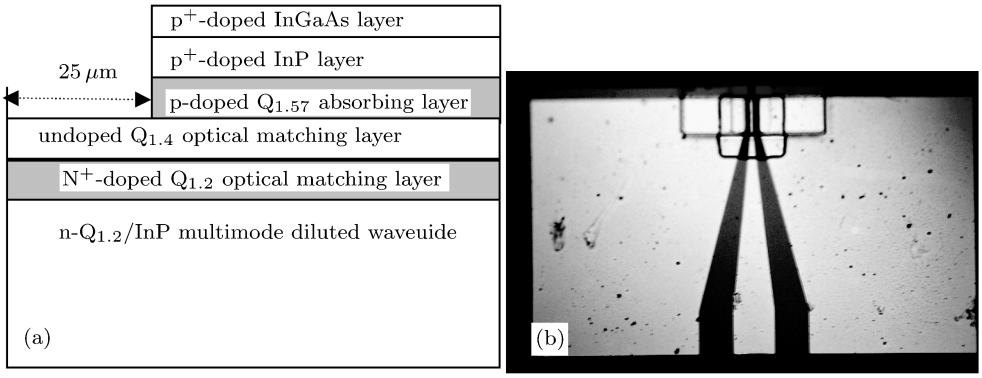


Fig.1. (a) Schematic view and (b) top view of the demonstrated EC-UTC photodiode.

3. Bandwidth theory

The demonstrated EC-UTC PD shown in Fig.1(b) has a traveling wave electrical structure without matched termination at the optical input end. Therefore, to deal with the bandwidth constraint at the same time, we consider that the bandwidth performance of the EC-UTC PD is governed by three factors: (a) drift time in the undoped carrier collection layer; (b) diffusion time in the P-absorbing layer; and (c) the resistive-capacitive (RC) time constant.

The drift time $t_{\rm drift}$ to cross the undoped carrier collection layer can be expressed as

$$t_{\rm drift} \cong w_{\rm c}/v_{\rm e}, \tag{1}$$

where $v_{\rm e}$ and $w_{\rm c}$ are the average electron speed and the thickness of the undoped carrier collection layer.

The average diffusion time of the electrons, $t_{\rm diff}$, in this P-absorbing layer can then be obtained as[13]

$$t_{\rm diff} \approx \frac{w_{\rm a}^2}{2D_{\rm e}} + \frac{w_{\rm a}}{v_{\rm th}}, \tag{2}$$

where $v_{\rm th}$ and $D_{\rm e}$ are the electron thermionic emission rate and the electron diffusion coefficient in the P-absorbing layer, respectively.

Take into account the ballistic travel of the electrons, which substantially reduces the transit time, and assume that electrons move in the undoped carrier collection layer at an overshoot speed ($v_e = 2 \times 10^7$ cm/s),[14,15] and that D_e and v_{th} are 150 cm^2/Vs and 2.5×10^7 cm/s, respectively, then the drift time and the diffusion time of the demonstrated EC-UTC photodiode with $w_c = 0.3$ μm and $w_a = 0.15\,\mu$m will be estimated to be approximately 1.5- and 1.35-ps, respectively.

For the RC bandwidth, we use a standard small signal equivalent circuit model with 50-Ω load resistance (R_L). The f_{RC} of the EC-UTC TWPD can be expressed as

$$f_{RC} = \frac{1}{2\pi C(R_s + R_L)}. \tag{3}$$

Therefore, the theoretical approximate 3-dB frequency is obtained as follows:[16]

$$f_{3dB} = \frac{f_t}{\sqrt{1 + \left(\frac{f_t}{f_{RC}}\right)^2}}, \tag{4}$$

where f_t is 3-dB transit time frequency determined by drift time in the undoped carrier collection layer and diffusion time in the P-absorbing layer; f_{RC} is the bandwidth restricted by the RC time constant.

Figure 2 shows the calculated 3-dB bandwidth and RC bandwidth of the demonstrated EC-UTC PD with $w_c = 0.3\,\mu$m and $w_a = 0.15$ μm as a function of diode length for a fixed diode width of 6 μm. The solid circle shown in Fig.2 denotes the 3-dB transit time frequency (f_t = 56 GHz) of the demonstrated

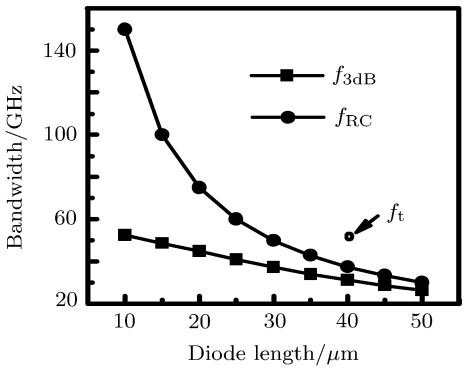


Fig.2. Calculated f_{RC} and f_{3dB} of the demonstrated EC-UTC PD with $w_a = 0.15$ μm, and $w_c = 0.3$ μm as a function of diode length for a fixed diode width of 6 μm.

EC-UTC PD with $w_c = 0.3$ μm and $w_a = 0.15$ μm. According to Fig.2, when the length is larger than 30 μm, f_{3dB} is CR limited. But when the length is reduced, the bandwidth tends to be saturated, which means that the f_{3dB} value is limited to the carrier transit time.

4. Optical and electrical characteristics

This structure was studied by using a three-dimensional beam propagation method (3-D BPM). The employed optical refractive indexes and optical absorption constants of InGaAsP quaternaries used in the BPM for optical waveguide simulation can be found in Ref.[17]. A tunable semiconductor laser was employed as a light source for dc photocurrent measurement. The central wavelength of this laser was fixed at 1550 nm during dc measurement. The measured and the simulated responsivities versus the length of the diode are shown in Fig.3. A responsivity of 0.36 A/W was obtained with a 6×40 μm^2 diode. Longer devices (50 μm) exhibited higher responsivity (0.39 A/W). The measured responsivity was lower than that simulated by using the BPM (0.63 A/W for a 6×40 μm^2 diode). This discrepancy could result from the scattering loss at the deeply dry-etched waveguide facets and reflection loss from the front of the passive waveguide in the fabricated devices. By using anti-reflection (AR) coating, the responsivity of the photodiode is expected to be greatly improved.

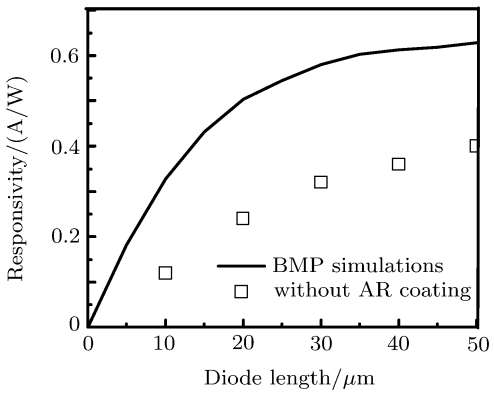


Fig.3. Responsivities measured at –2 V reverse-bias voltage and simulated by using 3D-BPM at 1550 nm wavelength versus diode length (with width=6 μm).

As shown in Fig.3, the 3-dB frequency of the demonstrated EC-UTC photodiode (with diode length=40 μm) was estimated to be 37 GHz and the RC time constant was a dominant factor of the restricting 3-dB bandwidth. The bandwidths were measured by using a spectrum analyzer. Figure 4

shows a schematic of the experimental setup used to characterize the EC-UTC photodiodes. A tunable laser coupled into a lithium niobate Mach–Zehnder modulator (MZM) generated a swept frequency optical sinusoid signal. An erbium-doped fiber amplifer (EDFA) subsequently amplified the optical signal. An attenuator (ATTN) combined with a fiber power meter could be used to accurately set the power of the optical beam which was incident on the EC-UTC photodiode. The electrical output of the detector was connected with a spectrum analyzer by using a coplanar probe connected to a short coaxial cable and an external bias tee (bias T). Figures 5 and 6 show the measured and fitted small signal frequency responses of the device with a 40 μm active area at reverse-bias voltages of 2 V and 4 V, respectively. The straight lines denote polynomial fits. The bandwidths for 6×40 μm^2 photodiode can reach 10 and 11.5 GHz at reverse-bias voltages of 2 V and 4 V, respectively. These measured bandwidths are much shorter than the calculated bandwidth (37 GHz), because the measurement setup was not calibrated to eliminate the radio frequency (RF) losses induced by the components, especially the coaxial cables used for measurement at the frequencies equal to and lower than 10 GHz. The measured RF bandwidth can be greatly improved by eliminating RF losses induced by the probe and the bias tee between the photodiode and a spectrum analyzer and by using new coaxial cables (capable of performing the 40 GHz measurement). In addition, it is noteworthy that the bandwidth at –4 V is smaller than at –2 V as shown by a comparison between Figs.5 and 6. This difference should be attributed to the increase of the drift time of the electrons in the un-doped carrier collection layer at a higher bias voltage because the speed overshoot in the InP collector layer appears more clearly at lower potential differences over the traveling distance.[4]

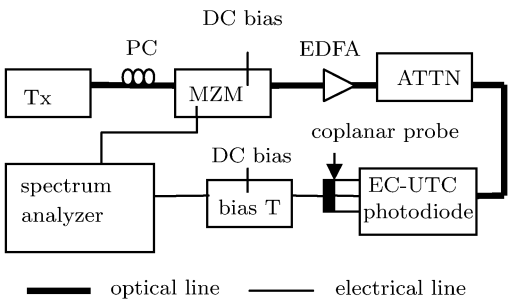


Fig.4. Measurement setup for testing EC-UTC photodiodes.

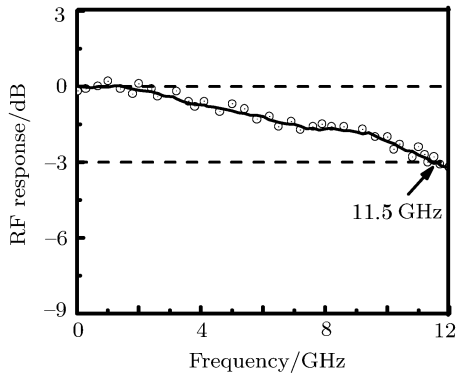


Fig.5. Bandwidth response of a 6×40 μm^2 EC-UTC photodiode at a reverse-bias voltage of 2 V, where the open circles denote the measurements and the solid line represents a polynomial fit.

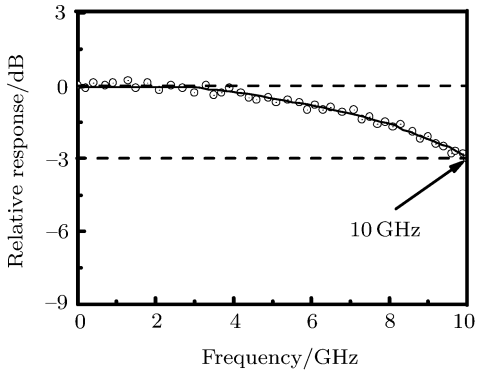


Fig.6. Bandwidth response of a 6×40 μm^2 EC-UTC-PD at a reverse-bias voltage of 4 V, where the open circles denote the measurements and the solid line represents a polynomial fit.

Regarding the high optical power behaviour of the EC-UTC PD, traces shown in Fig.7 represent the photogenerated radio-frequency (RF) power versus dc photocurrent of the EC-UTC PD at reversebias voltages of 3 V and 4 V. The operating frequency was fixed at 10 GHz. According to Fig.7, the –1-dB compression points at 10 GHz are corresponding to 11 and 18 mA, respectively. A maximum saturation current of 18 mA for the 240-μm^2 device at 10 GHz is obtained at a reversebias voltage of 4 V. The result reported here demonstrates that the EC-UTC photodiode provides a higher saturation current and lower operation voltage, thereby leading to power consumption at equal currents. This demonstrates that the EC-UTC photodiode has been improved significantly in optical power capacity.

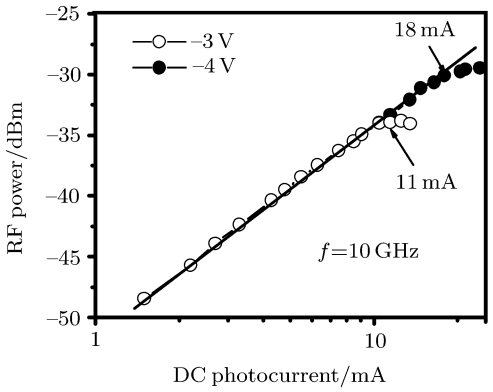


Fig.7. RF power versus dc current at 10 GHz, with reverse-bias voltages being –3 V and –4 V and the size of the diode being 6×40 μm^2.

5. Conclusion

In this paper, a new evanescently-coupled uni-traveling-carrier photodiode (EC-UTC-PD) based on a multimode diluted waveguide (MDW) structure is made and analysed with the aim of achieving a high saturation current. It is found that when the length of the demonstrated EC-UTC-PD is larger than 30 μm, the RC time constant is the dominant factor of the restricting 3-dB bandwidth. A 4×60 μm^2 EC-UTC-PD has achieved a responsivity of 0.36 A/W at 1550 nm wavelength, a bandwidth of 11.5 GHz and small-signal 1-dB compression current greater than 18 mA at 10 GHz. The RF bandwidth can be further improved by eliminating RF losses induced by the probe and the bias tee between the photodiode and the spectrum analyzer, especially the coaxial cables. The saturation current is significantly improved compared with those of similar evanescently coupled pin photodiodes.

Acknowledgement

The authors would like to thank Wang Bao-Jun, Zhou Fan, Pan Jiao-Qing and Shu Hui-Yun for their help with the experiment, and also Wang Lu-Fong, Bian Jing and An Xin for the device test.

References

[1] Ishibashi, T Furuta and Fushimi T H 2000 *IEICE Trans. Electron.* **E83-C** 938
[2] Ishibashi T, Kodama S and Shimizu N 1997 *Jpn. J. Appl. Phys.* **36** 6263
[3] Ishibashi T, FurutaT and Fushimi H 2001 *Proc. SPIE.* **4283** 469
[4] Shimizu N, Watanabe N and Furuta T 1998 *IEEE Photon. Technol. Lett.* **10** 412
[5] Kato K, Kozen A, Muramoto Y, Itaya Y, Nagatsuma T and Yaita M 1994 *IEEE Photon. Technol. Lett.* **6** 719
[6] Demiguel S, Giraudet L, Joulaud L, Decobert J, Blache F, Coupé F, Jorge F, Pagnod-Rossiaux P, Boucherez E, Achouche M and Devaux F 2002 *J. Lightwave Technol.* **12** 2004
[7] Achouche M, Demiguel and Derouin E 2003 *Proc. Optical Fiber Communication Conf.* 23
[8] Magnin V, Giraudet L and Harari E 2002 *J. Lightwave Technol.* **20** 477
[9] Demiguel S, Giraudet L and Joulaud L 2002 *J. Lightwave Technol.* **20** 2004
[10] Bach H G, Beling A, Mekonnen, G and Kunkel G 2004 *IEEE J. Sel. Top. Quantum Electron.* **10** 668
[11] Liao Z Y, Yang H and Wang W 2008 *Chin. Phys.* B **17** 2557
[12] Demiguel S, Li N, Li X, Zheng X, Kim J, Campbell G C, Lu H and Anselm A 2003 *IEEE Photon. Technol. Lett.* **15** 1761
[13] Size S M 1998 *Modern Semiconductor Device Physics* (New York: John Wiley & Sons) Chapter 1
[14] Ishibashi T 1994 *Semiconductors and Semimetals* (San Diego, CA: Academic) 333
[15] Madjar A, Peter R, Herczfeld, Rosen A, Paul Yu and Dieter J 2005 *Microwave Conference* **1** 3
[16] Giboney K S, Rodwell M J W and Bowers J E 1997 *IEEE Trans. Microwave Theory Tech.* **45** 1310
[17] Levinshtein M, Rumyantsev S and Shur M 1996 *Handbook Series on Semiconductor Parameters* (Singapore: World Scientific)